

# NUMERICAL INVESTIGATION OF STRUCTURAL AND STATISTICAL FEATURES OF PREMIXED FLAME UNDER INTENSE TURBULENCE

R. Ranjan and S. Menon

School of Aerospace Engineering  
Georgia Institute of Technology  
270 Ferst Drive, Atlanta, GA, 30332, USA  
reetesh.ranjan@ae.gatech.edu, suresh.menon@ae.gatech.edu

## ABSTRACT

In this study results from large-eddy simulation (LES) employing the linear eddy mixing (LEM) model of a freely propagating methane/air turbulent premixed flame interacting with a decaying background turbulence field are analyzed to characterize the effects of Karlovitz number ( $Ka$ ) ranging from 30 to 120 on the flame-turbulence interaction. The analysis is performed in terms of the resolved and the subgrid-scale (SGS) flame structure, by examining the instantaneous snapshots, spatially averaged profiles, propagation characteristics, and statistical features of the flame. The LES predicts the turbulence-chemistry interaction at high  $Ka$ , as in direct numerical simulation (DNS) and experimental studies. In particular, the effects of increased  $Ka$ , which results in enhanced mixing and homogenization within the flame region are captured in the simulations, thus providing confidence that LEM model has the potential to capture a wide range of operating conditions encompassing thin reaction zone to broken/distributed reaction zone regimes without requiring any model adjustment.

## INTRODUCTION

Turbulent premixed combustion is observed in several combustion devices such as internal combustion engines, gas turbines, and swirl combustors. Such systems are typically operated under lean conditions, however, the lean conditions lead to a slow propagation of flames, thus necessitating operation of the device under intense turbulence conditions to allow for a stable combustion (Strakey *et al.*, 2007). A key feature of flames under intense turbulence is the modification of the flame structure, particularly, the preheat zone (Zhou *et al.*, 2017; Wabel *et al.*, 2017a; Ranjan *et al.*, 2016). It is also hypothesized that at extreme levels of turbulence, the reaction zone may get disrupted leading to a local/global extinction (Peters, 2000). The turbulence-chemistry interaction observed in such flames is a multi-scale phenomenon, where the interplay of various processes such as reaction, diffusion, convective processes and thermal expansion occurring within flame region becomes important. Therefore, any modeling of turbulence-chemistry interaction should be able to capture the wide range of physics in a robust, consistent and accurate manner without requiring *ad hoc* model adjustments. In this study, LES based investigation of a freely propagating turbulent premixed flame is performed to analyze the effects of increased turbulence intensity on the resolved and the SGS

features of the flame.

Turbulent premixed flames are classified into different regimes, which are referred as wrinkled flamelets (WF), corrugated flamelets (CF), thin reaction zone (TRZ) and broken/distributed reaction zone (B/DRZ) (Peters, 2000). Recent experimental studies have characterized another regime, referred as broadened preheat-thin reaction (BP-TR) layer for flames under extreme turbulence (Wabel *et al.*, 2017b). The key parameters for classification of premixed flame regimes are: turbulence intensity ( $u'$ ), laminar flame speed ( $S_L$ ), integral length scale ( $l$ ), and Zeldovich flame thickness ( $\delta$ ). These regimes can also be characterized in terms of other non-dimensional numbers, namely Karlovitz number ( $Ka = \sqrt{u'^3 \delta / S_L^3 l}$ ), Reynolds number ( $Re_L = u' l / \nu$ ) and Damköhler number ( $Da_L = S_L l / u' \delta$ ). A higher value of  $Ka$  is typically associated with an intense turbulence, where smaller and energetic turbulent eddies can penetrate within the flame region and disrupt its structure (Peters, 1999; Sankaran *et al.*, 2007; Ranjan *et al.*, 2016; Wabel *et al.*, 2017b,a). Recent studies of flames under intense turbulence show presence of features such as broadening of preheat zone, thin reaction layer with no effects of turbulent eddies on them, and bending of the consumption speed curve with respect to the turbulence intensity (Wabel *et al.*, 2017b,a).

The focus of this study is to analyze the resolved and the SGS features of premixed flame under intense turbulence by using the LEM model within the LES framework (LEMLES) (Menon & Kerstein, 2011). LEMLES is a multi-scale formulation for scalar transport and mixing, and allows for handling arbitrary finite-rate chemistry effects. The analysis is performed in terms of structural and statistical features of the turbulent premixed flame to assess if the model can capture the characteristic features of such flames in a consistent manner, which has been reported in past numerical and experimental studies.

## PROBLEM DESCRIPTION AND NUMERICAL METHODOLOGY

The reacting flow configuration considered in this study corresponds to the interaction of an initially planar lean premixed methane-air flame with an initially intense and decaying turbulent flow field. The initial laminar flame solution is obtained at  $\phi = 0.8$ ,  $T_{ref} = 570$  K and  $P_{ref} = 1$  atm, and is superimposed over a background turbulent flow field with flame positioned near the center of the com-

Case	$u'/S_L$	$Re$	$Ka$	$Da$
$Ka^{30}$	20.4	191	30	0.46
$Ka^{60}$	32.4	302	60	0.29
$Ka^{90}$	42.4	396	90	0.22
$Ka^{120}$	51.4	480	120	0.18

Table 1. Initial turbulent premixed flame parameters for all cases.

putational domain with reactants and products on its left and right sides, respectively. The flow field is initialized using an isotropic flow field by using the Kraichnan spectrum (Kraichnan, 1970), followed by evolving the turbulence to a physical state till one eddy turnover time ( $\tau = u'/l$ ), and rescaling  $u'$  to match the initial  $Re$ . To analyze the effects of an increase in  $Ka$  on the structural and statistical features of the flame-turbulence interaction, a parametric study is conducted by fixing the length-scale ratio ( $l/\delta = 9.4$ ) and varying  $Ka$  from 30 to 120. The parameters for the four cases considered in this study are shown in Table 1, where the cases are denoted by  $Ka^m$ , with  $m = 30$  indicating the value  $Ka$ . A reduced four-step and eight species ( $\text{CH}_4$ ,  $\text{O}_2$ ,  $\text{N}_2$ ,  $\text{CO}$ ,  $\text{CO}_2$ ,  $\text{H}$ ,  $\text{H}_2\text{O}$ ,  $\text{H}_2$ ) methane-air mechanism with finite-rate kinetics (Peters, 1991), temperature dependent properties, and non-unity Lewis numbers is used in this study. Based on the initial conditions, case  $Ka^{30}$ ,  $Ka^{60}$ , and  $Ka^{90}$  corresponds to the TRZ regime, whereas  $Ka^{120}$  corresponds to the B/DRZ regime.

The extent of the computational domain is  $2L \times L \times L$  in the streamwise ( $x$ ), transverse ( $y$ ) and spanwise ( $z$ ) directions, where  $L = 0.0055$  m. The spatial discretization utilizes  $256 \times 128 \times 128$  uniform sized cells for LES, and 12 LEM cells are used at the subgrid level. Additional simulations with refined LES and LEM resolutions (not discussed here) do not affect the statistics discussed here, and therefore, the grid used in this study is considered to be adequate. A characteristic based inflow-outflow boundary condition is used in the  $x$  direction and periodic boundary condition is used along the  $y$  and  $z$  directions.

The unsteady Favre-filtered multi-species compressible Navier-Stokes equations are solved using a three-dimensional parallel finite volume solver, which is formally second-order accurate in space and time. The subgrid-scale (SGS) momentum and energy fluxes are closed using a subgrid eddy viscosity, that employs the turbulent kinetic energy for which an additional transport equation is solved, with model coefficients determined through a dynamic procedure (Kim & Menon, 1999). The turbulence-chemistry interaction at the SGS level is closed using the LEM model (Menon & Kerstein, 2011). The LEM model acts as an embedded SGS model for the species equation as viewed on the LES space and timescale, and therefore, it models the scalar mixing processes occurring at the molecular level, which can not be resolved on the LES grid. The processes involved in the scalar evolution using LEM includes the molecular diffusion, turbulent convection by the eddies, and chemical reaction for the species at their respective spatial and temporal scales. Further details about the computational setup, governing equations, and closure models are discussed in Ranjan *et al.* (2016).

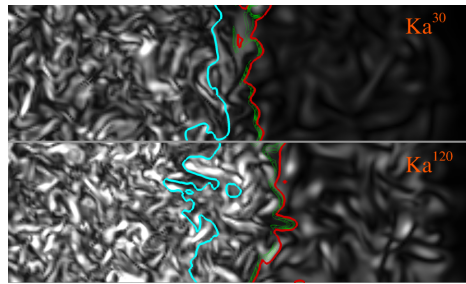


Figure 1. Contours of vorticity magnitude in the central  $x - y$  plane overlaid with the flame brush extents identified by  $\tilde{c} = 0.01$  (cyan color) and  $\tilde{c} = 0.99$  (red color). The reaction zone is identified by green colored contours of heat release rate.

## RESULTS

### Structural Features of Flame

The flame-turbulence interaction is analyzed in terms of the effect of  $Ka$  on the flame structure and the vorticity magnitude field, which are shown in Fig. 1 for cases  $Ka^{30}$  and  $Ka^{120}$ . The flame brush is identified using the value of resolved progress variable  $\tilde{c} \in [0.01, 0.99]$ , where  $\tilde{c} = (\tilde{Y}_{F,u} - \tilde{Y}_F) / (\tilde{Y}_{F,u} - \tilde{Y}_{F,b})$ . Here,  $\tilde{Y}_F$  denotes the fuel (methane) mass fraction of the fuel, and subscripts ‘u’ and ‘b’ denote its value in the reactants and the products sides, respectively. The reaction zone is identified through the contours of the heat-release-rate field. With an increase in  $Ka$ , the width of the flame brush increases, which is consistent with past studies of such flames (Dunn *et al.*, 2009; Savre *et al.*, 2013; Aspden *et al.*, 2011; Srinivasan & Menon, 2014; Wabel *et al.*, 2017b). The intense turbulent eddies lead to a fine-scale distortion of the flame brush, particularly evident at higher  $Ka$ . Along the  $y$ -direction, the flame brush width varies due to the straining effect of the large-scale eddies. The effect of flame on the turbulence is apparent from the decay of the vorticity field in both the cases, which is accompanied with an increase in the length-scale in the post-flame region. The effect of homogenization due to eddies penetrating the flame brush region is particularly noticeable in case  $Ka^{120}$ , where protruding structures at the boundaries of the flame brush appear on both reactants and products sides. Such structures are associated transport of heat away from the reaction zone and unburnt fuel close to the reaction zone by the turbulent eddies. The reaction zone remains continuous in all the cases, thus precluding the existence of a broken reaction zone for the cases considered in this study.

The effect of  $Ka$  on the global flame structure is examined in terms of the spatially averaged quantities, which are shown in Fig. 2. The averaging is performed along the homogeneous  $y$ - and  $z$ -directions through:  $\langle q \rangle(\xi, t) \equiv \frac{1}{L^2} \int_0^L \int_0^L q(x - x_0(t), y, z) dy dz$ . Here,  $\xi = x - x_0(t)$  is a modified streamwise coordinate, which moves with the global flame position  $x_0(t)$ , defined as:  $x_0(t) \equiv \frac{1}{L^2 (\bar{\rho} \tilde{Y}_F)_u} \int_V \bar{\rho} \tilde{Y}_F dV$ . The spatially averaged quantities are obtained at  $t^* = t/\tau = 3$ , where  $\tau$  is the initial eddy turnover time. With an increase in  $Ka$ , a progressive broadening in the profile of the progress variable is evident consistent to the instantaneous flame structure shown in Fig. 1. Additionally, the profiles show the presence of mixed partially burned and unburned fluid ahead of the reaction zone. As  $Ka$  is increased, the enhanced mass and heat transport leads to homogenization

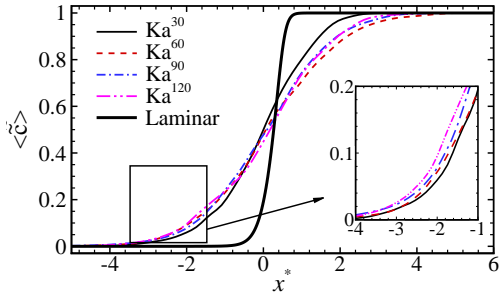


Figure 2. Profile of the spatially averaged progress variable for all cases at  $t^* = 3$ . Here  $x^* = (x - x_0)/\delta_L$  is the non-dimensional spatial coordinate.

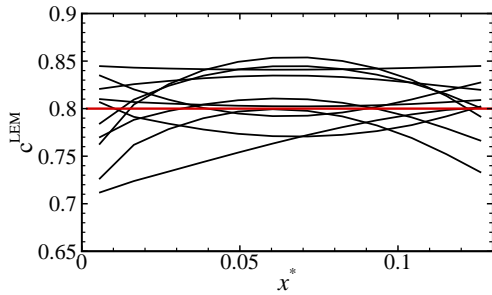


Figure 3. SGS variation of progress variable ( $c^{LEM}$ ) embedded within the LES cells with  $\tilde{c} = 0.8$  for case  $Ka^{120}$ . For sake of clarity only 10 LEM profiles are included.

within the flame brush, which decreases the gradient of the progress variable. Furthermore, the enhanced transport by the turbulent eddies also leads to a reduction in the consumption of the fuel, as evident from a wider distribution of the progress variable compared to a sharp front observed in the laminar solution. These features are also observed in past studies of such flames (Aspden *et al.*, 2011; Srinivasan & Menon, 2014; Wabel *et al.*, 2017b). With an increase in  $Ka$  the mean flame brush thickness increases by about 20% from case  $Ka^{30}$  to case  $Ka^{120}$ , whereas the reaction zone thickness remains nearly constant, thus implying that the eddies approaching the reaction zone get dissipated leading to a continuous and thin reaction layer (Wabel *et al.*, 2017a).

Since the LEMLES formulation is a multi-scale approach for the species transport and mixing, therefore, the SGS characteristics of the flame can be examined. The SGS information about the scalar field apart from providing means to analyze the consistency of predictions at the resolved level, also allows to assess if a model reduction for certain class of problems is feasible. To facilitate analysis of the SGS fields, solutions of the scalar field from the 1D-LEM domain are extracted corresponding to the representative LES resolved flame surface identified by  $\tilde{c} = 0.8 \pm 0.02$ . Fig. 3 shows the SGS variation of the progress variable ( $c^{LEM}$ ) for case  $Ka^{120}$ . The value of  $c^{LEM}$  varies by about 30% from the corresponding value at the resolved level, thus demonstrating the role of intense turbulence, which distorts the flame surface. The amount of variation of the progress variable is higher in the preheat zone, which is due to homogenization by the turbulent eddies discussed above. In addition, multiple flame crossings are observed at the LEM level, which is consistent with the intense wrinkling

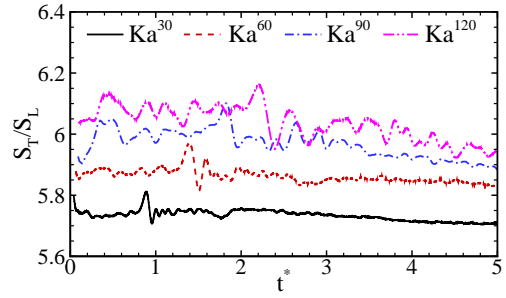


Figure 4. Time evolution of the normalized turbulent flame speed ( $S_T/S_L$ ) for all the cases.

of the flame surface at higher  $Ka$  (Peters, 2000; Sankaran & Menon, 2005; Aspden *et al.*, 2011; Srinivasan & Menon, 2014). These results demonstrate that the LEM employed at the SGS is able to capture the enhanced mixing and transport induced by the small-scale turbulent eddies.

The effect of  $Ka$  on the propagation of the flame is characterized in terms of turbulent flame speed, which is shown in Fig. 4 and defined in terms of the consumption speed through:  $S_T(t) = U_{ref} - \frac{dx_0(t)}{dt}$ , where  $U_{ref}$  is the bulk inflow velocity and  $x_0(t)$  is the spatially averaged flame location. The turbulent flame speed is a global quantity, which specifies the mean speed at which reactants must be provided to keep the position of the flame front statistically stationary. With an increase in  $Ka$ , an increase in  $S_T/S_L$  occurs where a quasi-stationarity value is reached in all cases for  $t^* \in (0.5, 3)$ . Afterward, as the turbulence intensity upstream of the flame region decreases, the flame speed reduces in all the cases. The time-averaged value of the flame speed ( $\overline{S_T}/S_L$ ) where averaging is performed for  $t^* \in (0.5, 3)$  is shown in Table 2, where it can be observed that the flame speed increases in a non-linear manner with increase in  $Ka$  showing the well known ‘‘bending behavior’’, where the value of the flame speed saturates with increase in the value of turbulence intensity.

An alternate way to characterize, the propagation of a turbulent premixed flame is in terms of the wrinkling factor, which is defined as:  $\Xi(t) = A(t^*)/A(0)$ , where  $A(t^*)$  denotes the flame front area at time  $t^*$  corresponding to  $\tilde{c} = 0.8$ . Due to stretching and wrinkling effects of the turbulent eddies, the flame surface area increases and reaches a quasi-stationary value for  $t^* \approx 3$ . The value of  $\Xi$  is summarized in Table 2, which varies from about 2.7 to 3.2 across different cases. It is apparent that the magnitude of the normalized flame propagation speed shown in Fig. 4 differs from the wrinkling factor, which can be attributed to the effect of enhanced transport, which is included in the flame propagation speed in addition to the increased flame surface area. Therefore, a closure model for turbulent flame speed can not be solely based on the wrinkling factor.

Further structural features of the flame are quantified in terms of the resolved curvature ( $\kappa$ ), mean flame brush thickness ( $\delta_m$ ) and mean reaction zone thickness ( $\delta_{0.5}$ ), which are shown in Table 2. Here, curvature is defined as  $\kappa = \nabla \cdot n_{c=c_0}$ , where  $n = -\nabla c/|\nabla c|$  is the unit-normal vector pointing towards the reactants. A negative value of the curvature implies a concave flame with respect to the reactants. The PDF of  $\kappa\delta_L$  (not shown here) shows a positively skewed shape with mean value close to zero. The mean and skewness of  $\kappa$  decreases with increase in  $Ka$ , implying an

Case	$\mathcal{E}$	$\kappa\delta_L$	$\delta_m/\delta_L$	$\delta_{0.5}/\delta_{0.5,L}$	$\overline{S_T}/S_L$
$Ka^{30}$	2.7	0.5	5.5	1.6	5.7
$Ka^{60}$	3.2	0.3	7.6	1.5	5.9
$Ka^{90}$	3.1	0.1	7.1	1.7	6.0
$Ka^{120}$	2.9	0.1	6.7	1.5	6.1

Table 2. Statistics of the flame for all the cases at  $t^* = 3$ .

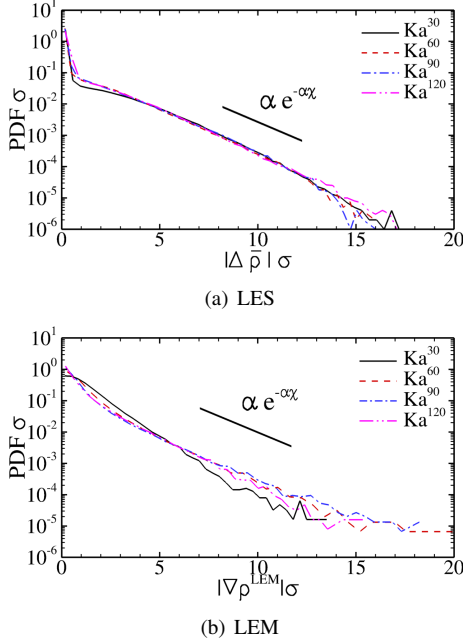


Figure 5. PDF of the density gradient magnitude at the resolved (a) and the subgrid (b) levels.

increasing effect of turbulent mixing, a characteristic feature of high  $Ka$  flames (Aspden *et al.*, 2011). The mean flame brush thickness is based on the bounding values of the progress variable, i.e.,  $0.01 \leq \langle \tilde{c} \rangle \leq 0.99$ , which represents the global flame thickness. The reaction zone thickness  $\delta_{0.5}$  is defined in terms of the thermal flame thickness corresponding to a specified value of the progress variable (De Goey *et al.*, 2005). It is apparent from Table 2 that while  $\delta_m$  increases with  $Ka$ ,  $\delta_{0.5}$  remains nearly constant. This is in agreement with the recent studies (Wabel *et al.*, 2017b,a) related to existence of BP-TR layer for premixed flames under intense turbulence.

### Statistical Features of Flame

The effects of  $Ka$  on the flame structure is now examined through single point statistics of the density gradient magnitude, and conditional statistics of temperature, the gradient of the progress variable, and fuel reaction rate with respect to the progress variable across the flame.

The structural changes to the flame surface can also be analyzed statistically in terms of the magnitude of density gradient, which is typically associated with the sharpness of the reactants/products interface. Figure 5 shows the PDFs of the density gradient magnitude at the resolved LES and the subgrid LEM levels. All of the cases show a similar be-

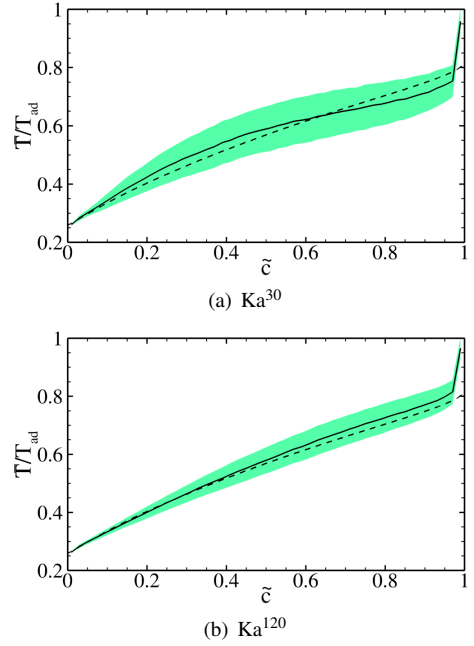


Figure 6. Conditional variation of the normalized temperature with respect to the progress variable. Solid and dashed curves denote the mean and laminar distribution, respectively. The shaded region correspond to the standard deviation about the mean distribution.

havior, where the normalized PDFs approach an exponential distribution, which is given by:  $f(\chi; \alpha(t)) = \alpha e^{-\alpha(t)\chi}$ , where  $\chi \equiv |\nabla \tilde{c}|$  is the state-space variable and  $\alpha(t)$  is the inverse scale. The approach of the PDF of density gradient magnitude at high  $Ka$  to an exponential distribution is similar to that reported in the past DNS based study of flames under D/BRZ conditions (Aspden *et al.*, 2011). A key feature to notice is that this behavior of the PDF is also observed at the subgrid level, thus demonstrating the unique ability of the LEMLES formulation to capture features of flames under intense turbulence conditions at both the resolved and subgrid levels. With an increase in  $Ka$ , the SGS variation of density gradient magnitude decreases, which occurs due to the effect of homogenization as discussed above and evident in Fig. 1.

Figure 6 show the conditional variation of  $\overline{T}/T_{ad}$  with respect to  $\tilde{c}$  for cases  $Ka^{30}$  and  $Ka^{120}$  at  $t^* = 3$ . A reference curve corresponding to the laminar flame distribution is also included for comparison. The increase in the turbulent mixing has two major effects. First, the mean profile deviates away from the laminar distribution towards higher temperature and second, the standard deviation of the temperature field reduces. The mean distribution of temperature remains closer to the unstretched laminar flame distribution in case  $Ka^{30}$ , however, regions of hot spots and a de-correlation of temperature with the progress variable are also observed, implying preheating of the fuel compared to the laminar flame. This occurs due to a dominance of differential/molecular diffusion effects at lower  $Ka$  (Day *et al.*, 2009). However, in case  $Ka^{120}$  distribution appears to be narrower and shows a quasilinear behavior. The narrower distribution in high  $Ka$  premixed flames occurs due to the effects of stretch and chemical kinetics (Mansour *et al.*, 1992; Dunn *et al.*, 2009). A shift in the mean distribution from the laminar distribution towards higher temperature,

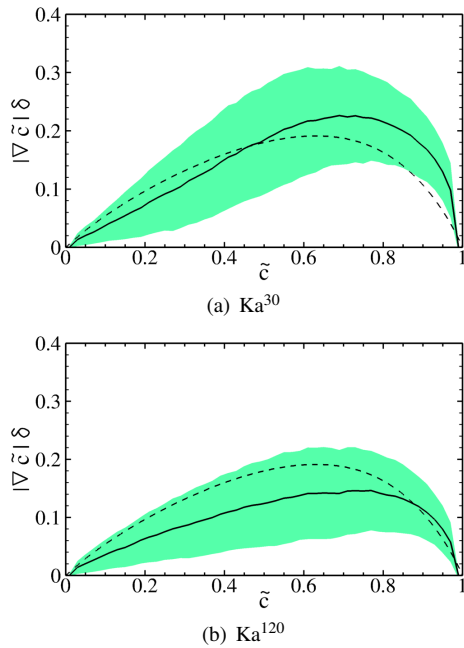


Figure 7. Conditional variation of the normalized progress variable gradient magnitude with respect to the progress variable. Solid and dashed curves denote the mean and laminar distribution, respectively. The shaded region correspond to the standard deviation about the mean distribution.

particularly across the flame and post-flame regions is observed, which is a well-known feature of high  $Ka$  flames, where turbulent micro-mixing become significant or even dominant over differential diffusion, leading to a deviation in the mean distribution from the distribution observed in laminar flames (Day *et al.*, 2009; Aspden *et al.*, 2011). From these results, the competing effects of molecular and turbulent mixing as  $Ka$  is increased is apparent, where the transition from molecular mixing dominated flame to turbulent mixing dominate flame from case  $Ka^{30}$  to case  $Ka^{120}$  is apparent, which further demonstrate the ability of the LEM-LES formulation to accurately predict behavior of flames where transitional regime could be observed.

The magnitude of the progress variable gradient  $|\nabla\tilde{c}|$  can be used as another measure of the flame thickness in a manner analogous to the thermal flame thickness  $\delta_L$ . Figure 7 shows the variation of  $|\nabla\tilde{c}|$  with respect to  $\tilde{c}$ . In the preheat zone, in both cases the mean values are lower than the corresponding laminar values, thus implying a broadening of the flame. However, the reaction zone observes a thinning in case  $Ka^{30}$  that transform to a thickening in case  $Ka^{120}$ . The effect of enhanced transport with increase in  $Ka$  is also evident in form of a decrease in the deviation about the mean distribution (Aspden *et al.*, 2011; Savre *et al.*, 2013; Srinivasan & Menon, 2014).

LES of turbulent combustion comprises of closure problems for turbulent transport and filtered reaction-rate (Boger *et al.*, 1998; Poinso & Veynante, 2005), where the major efforts have been devoted in the past to modeling of the filtered reaction-rate term (Poinso & Veynante, 2005). In the LEMLES formulation, the SGS scalar transport is modeled through turbulent stirring approach whereas the reaction rate is represented in the 1D-LEM domain in a resolved manner. Based on the results presented in this study and other investigations of high  $Ka$  premixed flames (Asp-

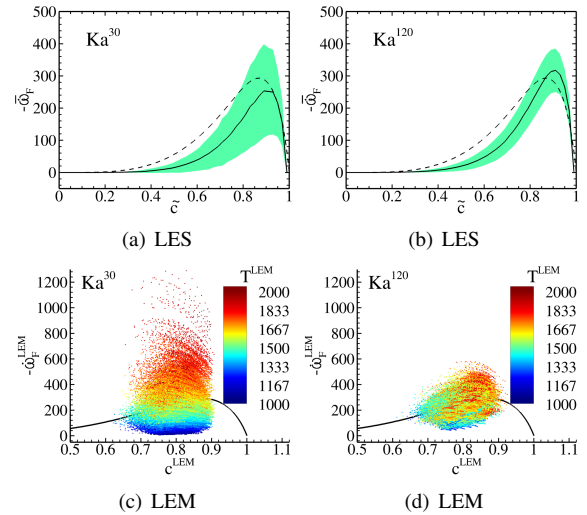


Figure 8. Conditional variation of the filtered fuel reaction rate term with respect to the progress variable (a, b) and scatter plot of the fuel reaction rate with respect to the progress variable at the LEM level (c, d).

den *et al.*, 2011; Savre *et al.*, 2013), it is observed that the role of turbulent mixing is dominant. Therefore, closure for the turbulent transport using a gradient diffusion approach seems to be reasonable for high  $Ka$  flames. Since the 1D-LEM domain contains a representation of the reaction-rate term, we examine the behavior of this term in comparison to the filtered reaction-rate term.

The structural changes to the flame brush region is analyzed in terms of the conditional variation of  $\omega_F$  with respect to  $\tilde{c}$ , which is shown in Fig. 8(a), and (b). The laminar distribution corresponding to the unstretched premixed flame solution is also included for reference. With an increase in  $Ka$ , the peak value of the mean distribution increases and the location of peak shifts toward higher values of  $\tilde{c}$ , or higher temperature. In addition, the standard deviation about the mean value decreases with an increase in  $Ka$  similar to that observed for conditional variation of temperature and progress variable gradient magnitude. In both cases, the mean distribution deviates away from the laminar distribution. However, the narrow distribution at high  $Ka$  implies that a conditioned reaction-rate closure can be attained for such flames (Sankaran *et al.*, 2007), where a reaction-rate conditioned with respect to the progress variable for strained laminar flames can be used along with a transport equation for the progress variable to attain a closure for turbulent premixed flames in the TRZ regime, which can lead to a simple and cost effective simulation of such flames in practical combustion devices.

Figure 8(c) and (d) show scatter plot of  $\omega_F$  with respect to  $\tilde{c}$  at the subgrid level. Similar to the resolved level, with an increase in  $Ka$ , the burning shifts towards higher values of temperature. Such a behavior of high  $Ka$  premixed flames is well-known (Aspden *et al.*, 2011; Savre *et al.*, 2013). Furthermore, a significant change in the variation of reaction-rate with an increase in  $Ka$  is observed, where the variation shifts from a broad distribution to a narrow distribution with an increase in  $Ka^{30}$ . Such a behavior of the reaction-rate at high  $Ka$  can be used to perform a simplified closure of the filtered reaction-rate term in conventional LES formulations.

## SUMMARY

LES based study of structural and statistical features of an initially planar, lean premixed methane-air flame interacting with an initially intense and decaying turbulence is performed to assess if features of such flames can be captured by using the LEM model for the SGS turbulence-chemistry interaction. Four cases are simulated by fixing the length-scale ratio and varying the velocity-scale ratio leading to variation of Karlovitz number from 30 to 120. Several of the key features of premixed flames under intense turbulence conditions are predicted with the LEMLES formulation consistent with the experimental and DNS findings at both resolved and subgrid levels.

The analysis of the instantaneous reacting flow features exhibit a significant disruption of the flame structure by the eddies, and dissipation of the small-scales due to thermal expansion. The spatially averaged profiles and statistics such as mean flame brush thickness and reaction zone thickness indicate the presence of a continuous flame structure with a broadened preheat zone and nearly constant width reaction layer at the resolved level, thus demonstrating the recent experimental findings of the broadened preheat-thin reaction layer regime. The increase in the flame propagation speed due to an intense turbulence is observed as expected, and the nonlinear variations of the turbulent flame speed with respect to the turbulence intensity are also predicted in agreement with past experimental studies.

The effect of  $Ka$  is examined in terms of single point statistics of the mean density gradient magnitude, and conditional statistics of the temperature, magnitude of the progress variable gradient, and fuel reaction rate. With an increase in  $Ka$ , the broadening of the flame brush region is accompanied by a corresponding reduction in the gradients of the field variable, which is associated with a dominance of the turbulence mixing over differential diffusion and molecular mixing effects. Additionally, the conditional variation with respect to the progress variable shows a narrow distribution at both resolved and subgrid levels, thus demonstrating the unique abilities of the LEMLES formulation to capture characteristic features of different regimes of the premixed combustion. The results presented in this study show that new cost-effective SGS models for real devices operating at high Reynolds number where grid resolution can not be refined can be developed. Such a study is currently underway.

## ACKNOWLEDGMENTS

This work is supported by AFOSR under a Phase II STTR from Combustion Science and Engineering, MD. The computational resources provided by the DOD HPC at the AFRL centers is greatly appreciated.

## REFERENCES

Aspden, A. J., Day, M. S. & Bell, J. B. 2011 Turbulence-flame interactions in lean premixed hydrogen: transition to the distributed burning regime. *J. Fluid Mech.* **680**, 287–320.

Boger, M., Veynante, D., Boughanem, H. & Trouve, A. 1998 Direct numerical simulation analysis of flame surface density concept for large eddy simulation of turbulent premixed combustion. *Proc. Combust. Inst.* **27**, 917–925.

Day, M. S., Bell, J. B., Bremer, P.-T., Pascucci, V., Beckner, V. E. & Lijewski 2009 Turbulence effects on cellular burning structures in lean premixed hydrogen flames. *Combust. Flame* **156**, 1035–1045.

De Goey, LPH, Plessing, T, Hermanns, RTE & Peters, Norbert 2005 Analysis of the flame thickness of turbulent flamelets in the thin reaction zones regime. *Proc. Combust. Inst.* **30**, 859–866.

Dunn, MJ, Masri, AR, Bilger, RW, Barlow, RS & Wang, G-H 2009 The compositional structure of highly turbulent piloted premixed flames issuing into a hot coflow. *Proc. Combust. Inst.* **32**, 1779–1786.

Kim, W. W. & Menon, S. 1999 An unsteady incompressible Navier-Stokes solver for large eddy simulation of turbulent flows. *I. J. for Numer. Meth. Fluids.* **31**, 983–1017.

Kraichnan, R. H. 1970 Diffusion by a random velocity field. *Physics of Fluids* **13**, 22–31.

Mansour, MS, Chen, YC & Peters, N 1992 The reaction zone structure of turbulent premixed methane-helium-air flames near extinction. In *Symposium (International) on Combustion*, , vol. 24, pp. 461–468.

Menon, S. & Kerstein, A. R. 2011 The linear-eddy model. *Turbulent Combustion Modeling* **95**, 175–222.

Peters, Norbert 1991 Reducing mechanisms. In *Reduced Kinetic Mechanisms and Asymptotic Approximations for Methane-Air Flames* (ed. M. D. Smooke), pp. 48–67. Springer.

Peters, N 1999 The turbulent burning velocity for large-scale and small-scale turbulence. *J. Fluid Mech.* **384**, 107–132.

Peters, N. 2000 *Turbulent Combustion*. Cambridge University Press.

Poinsot, T.J. & Veynante, D. 2005 *Theoretical and Numerical Combustion*, 2nd edn. Edwards, Inc.

Ranjan, R., Muralidharan, B., Nagaoka, Y. & Menon, S. 2016 Subgrid-scale modeling of reaction-diffusion and scalar transport in turbulent premixed flames. *Combust. Sci. Technol.* **188**, 1496–1537.

Sankaran, R., Hawkes, E. R., Chen, J. H., Lu, T. & Law, C. K. 2007 Structure of a spatially developing turbulent lean methane-air bunsen flame. *Proc. Combust. Inst.* **31**, 1291–1298.

Sankaran, V. & Menon, S. 2005 Subgrid combustion modeling of 3-D premixed flames in the thin-reaction-zone regime. *Proc. Combust. Inst.* **30**, 575–582.

Savre, J., Carlsson, H. & Bai, X. S. 2013 Turbulent methane/air premixed flame structure at high karlovitz numbers. *Flow Turbulence Combust.* **90**, 325–341.

Srinivasan, S. & Menon, S. 2014 Linear eddy mixing model studies of high karlovitz number turbulent premixed flames. *Flow Turb. Combust.* **93**, 189–219.

Strakey, P., Sidwell, T. & Ontko, J. 2007 Investigation of the effects of hydrogen addition on lean extinction in a swirl stabilized combustor. *Proc. Combust. Inst.* **31**, 3173–3180.

Wabel, T. M., Skiba, A. W. & Driscoll, J. F 2017a Turbulent burning velocity measurements: Extended to extreme levels of turbulence. *Proc. Combust. Inst.* **36**, 1801–1808.

Wabel, T. M., Skiba, A. W., Temme, J. E. & Driscoll, J. F 2017b Measurements to determine the regimes of premixed flames in extreme turbulence. *Proc. Combust. Inst.* **36**, 1809–1816.

Zhou, B., Brackmann, C., Wang, Z., Li, Z., Richter, M., Aldén, M. & Bai, X.-S. 2017 Thin reaction zone and distributed reaction zone regimes in turbulent premixed methane/air flames: Scalar distributions and correlations. *Combust. Flame* **175**.